HOKKAIDO UNIVERSITY

Title	Analysis of lead distribution in avian organs by LA-ICP-MS: Study of experimentally lead-exposed ducks and kites
Author(s)	Torimoto, Ryouta; Ishii, Chihiro; Sato, Hiroshi et al.
Citation	Environmental pollution, 283, 117086 https://doi.org/10.1016/j.envpol.2021.117086
Issue Date	2021-08-15
Doc URL	https://hdl.handle.net/2115/90295
Rights	©2021. This manuscript version is made available under the CC-BY-NC-ND 4.0 license http://creativecommons.org/licenses/by-nc-nd/4.0/
Rights(URL)	https://creativecommons.org/licenses/by-nc-nd/4.0/
Type	journal article
File Information	Environmental pollution283-117086.pdf

Hokkaido University Collection of Scholarly and Academic Papers

Hokkaido University Collection of Scholarly and Academic Papers : HUSCAP

TITLE: Analysis of lead distribution in avian organs by LA-ICP-MS: study of experimentally lead-exposed ducks and kites

AUTHORS: Ryouta Torimoto[a], Chihiro Ishii[b], Hiroshi Sato[b], Keisuke Saito[c], Yukiko Watanabe[c], Kohei Ogasawara[c], Ayano Kubota[d], Takehisa Matsukawa[d,e], Kazuhito Yokoyama[d,f], Atsushi Kobayashi[a,*], Takashi Kimura[a], Shouta M. M. Nakayama[b], Yoshinori Ikenaka[b,g], Mayumi Ishizuka[b]

* Authors to whom correspondence

AUTHOR ADDRESSES: [a]Laboratory of Comparative Pathology, [b]Laboratory of Toxicology, Faculty of Veterinary Medicine, Hokkaido University, Kita 18 Nishi 9, Kita-ku, Sapporo, Hokkaido 060-0818, Japan; [c]Institute for Raptor Biomedicine Japan, Hokuto 2-2101, Kushiro, Hokkaido 084-0922, Japan; [d]Department of Epidemiology and Environmental Health, [e]Department of Forensic Medicine, Juntendo University Faculty of Medicine, Hongo 2-1-1, Bunkyo-ku, Tokyo 113-8421, Japan; [f]Department of Epidemiology and Social Medicine, Graduate School of Public Health, International University of Health and Welfare, Akasaka 4-1-26, Minato-ku, Tokyo 107-8402, Japan; [g]Water Research Group, Unit for Environmental Sciences and Management, North-West University, Potchefstroom 2531, South Africa

CORRESPONDING AUTHORS:

Atsushi Kobayashi; Laboratory of Comparative Pathology, Faculty of Veterinary Medicine, Hokkaido University, Kita 18 Nishi 9, Kita-ku, Sapporo, Hokkaido 060-0818, Japan; e-mail kobayashi@vetmed.hokudai.ac.jp

ABSTRACT

Lead poisoning of wild birds by ingestion of lead ammunition occurs worldwide. Histopathological changes in organs of lead-intoxicated birds are widely known, and lead concentration of each organ is measurable using mass spectrometry. However, detailed lead localization at the suborgan level has remained elusive in lead-exposed birds. Here we investigated the detailed lead localization in organs of experimentally lead-exposed ducks and kites by laser ablation inductively coupled plasma mass spectrometry (LA-ICP-MS). In both the ducks and kites, lead accumulated diffusely in the liver, renal cortex, and brain. Lead accumulation was restricted to the red pulp in the spleen. With regard to species differences in lead distribution patterns, it is noteworthy that intensive lead accumulation was observed in the arterial walls only in the kites. In addition, the distribution of copper in the brain was altered in the lead-exposed ducks. Thus, the present study shows suborgan lead distribution in lead-exposed birds and its differences between avian species for the first time. These findings will provide fundamental information to understand the cellular processes of lead poisoning and the mechanisms of species differences in susceptibility to lead exposure.

KEYWORDS: Lead; LA-ICP-MS; imaging; waterfowl; raptor

MAIN FINDING: Suborgan lead distribution in experimentally lead-exposed birds and its species differences were revealed.

INTRODUCTION

The use of lead shots and bullets has been regulated in many countries. However, lead poisoning of wild birds is widespread all over the world (Pain *et al*., 2019). In the field, the ingestion of lead ammunition and fishing sinkers causes many cases of lead poisoning in waterfowls and raptors (Scheuhammer and Norris, 1996; Fisher *et al*., 2006; Saito, 2009). According to recent statistics, lead poisoning is estimated to kill annually a million waterfowls in Europe (Berny *et al*., 2015; Pain, 2019) and three million birds in the US (De Francisco *et al*., 2003). Lead poisoning in avian species has been recognized in Japan since 1985 (Honda *et al*., 1990), and endangered raptors in Japan have also been affected since 1996 (Saito, 2009). In birds, lead exposure exerts toxicity in various organs such as the liver, kidney, cardiovascular system, brain, and bone. The common gross lesions in birds are atrophy and brownish discoloration of the liver, distended gallbladder with bile, multifocal pallor areas in the myocardium, multifocal petechial hemorrhage in the cerebellum, and hypoplasia of the bone marrow (Ochiai *et al*., 1993; Manning *et al*., 2019). The histological lesions include hepatic hemosiderosis, degeneration and necrosis of the proximal renal tubules, degeneration and necrosis of myocardium, and cerebellar perivascular hemorrhage (Ochiai *et al*., 1993; Manning *et al*., 2019). Lead also interferes heme biosynthesis through the inhibition of the activities of δ-aminolevulinic acid dehydratase (ALAD) and ferrochelatase (Rogan *et al*., 1986; Fisher, 2006; Liao *et al*., 2008). Therefore, the diagnosis of avian lead poisoning is usually made by the characteristic histological changes, the level of ALAD activity in blood, and the lead concentration in blood and organs.

Lead concentration in organs is measurable by inductively coupled plasma-mass spectrometry (ICP-MS) using tissue homogenates (Ishii *et al*., 2017; Togao *et al*., 2020). In addition, special staining methods for lead in tissue sections have been developed to detect gunshot residues (Neri

et al., 2007; Turillazzi *et al*., 2013). However, the detailed lead distribution in lead-exposed animals at the suborgan level cannot be analyzed by these methods. Recently, we showed the tissue distribution of lead in lead-exposed mice using laser ablation (LA)-ICP-MS (Togao *et al*, 2020). LA-ICP-MS can identify metals in tissue sections and is useful to reveal the detailed tissue distribution of metals (Ek *et al.*, 2004; Ishii *et al*., 2018).

In the present study, we established a model of low-dose lead exposure in waterfowls and raptors by administration of one to three lead pellets, reproducing the low-dose lead exposure found in the field. Then, we investigated the histological distribution of lead in organs of the lead-exposed birds using LA-ICP-MS. In addition, we compared the tissue distribution of lead between waterfowls and raptors because the sensitivity to lead poisoning is reported to be different among avian species (De Francisco *et al*., 2003).

MATERIALS AND METHODS

Animal experiments

Animal experiments were performed in strict accordance with the Regulations for Animal Experiments and Related Activities at Hokkaido University. The protocols for animal experiments were approved by the Association for the Assessment and Accreditation of Laboratory Animal Care International and the Institutional Animal Care and Use Committee of Hokkaido University (approval No. 18-0092 and No. 19-0033).

Seven, bred, eight-week-old Muscovy ducks (*Cairina moschata*; body weight, 3.3 - 3.8 kg) were purchased from Sankyo Labo Service. The ducks were randomly divided into two groups; untreated control (n = 3) and lead-treated (n = 4). The ducks were housed individually in cages in controlled light (12 h light/dark cycle) and constant temperature (23 ± 2°C) with free access to

food and water. All ducks were acclimated for a week before treatment and kept on a fresh diet. Lead-treated ducks were given three lead pellets (240 ± 1.7 mg) in a style of oral forced ingestion. Control and lead-treated groups were euthanized with overdose of pentobarbital sodium on 29 or 30 days after the lead treatment.

Five black kites (*Milvus migrans*; body weight, 1.0 - 1.1 kg) were kept in the Institute for Raptor Biomedicine Japan. All kites were unsuitable for release because most had persistent wing damages. These kites were otherwise in good condition. The kites were placed individually in outdoor cages. Each pen was furnished with a log for perching and a pan of water. All kites were acclimated to the pens for a week or more before the treatment and were kept on a diet. The kites were randomly divided into two groups; untreated control (n = 2) and lead-treated (n = 3). Lead-treated kites were given one lead pellet (77.9 - 88.4 mg) mixed with venison. To confirm the existence of lead pellet in the gastrointestinal tract, the kites were radiographed every day for 14 days after the lead administration. In two kites (Kite-Lead-2 and Kite-Lead-3), the lead pellet disappeared on radiographs probably due to regurgitation or excretion at 7 and 10 days after the lead administration, respectively. Therefore, these kites were dosed one lead pellet again within 24 hours. Control and lead-treated groups were euthanized with overdose of pentobarbital sodium on 29 or 30 days after the first lead treatment.

Blood collection

Blood samples (5 ml and 4 ml from the ducks and kites, respectively) were obtained from the brachial veins at 28 days after the lead treatment. Blood was quickly heparinized to avoid coagulation and kept on ice until further processing within 2 hours.

Tissue sample collection

Liver, spleen, kidney, heart, lung, cerebrum, midbrain, cerebellum, and bone marrow were collected from the euthanized birds and divided into three pieces. One was used for quantitative analysis of lead by ICP-MS, another was used for histopathological analysis, and the other was used for imaging analysis of lead by LA-ICP-MS.

Quantitative analysis of lead by ICP-MS

Analyses of lead concentrations in bird organs (liver, spleen, kidney, heart, cerebrum, midbrain, cerebellum, and blood) were performed as reported previously (Yabe *et al*., 2015). The amounts of samples analyzed are summarized in Appendix A: Table A.1. Samples were digested with nitric acid (HNO_3) and hydrogen peroxide (H_2O_2) in microwave. The concentration of lead was measured with ICP-MS 7700 series (Agilent Technology). Analytical quality control was performed using DOLT-4 (dogfish liver) and DORM-3 (fish protein) (National Research Council of Canada) certified reference materials. Replicate analyses of these reference materials showed good recoveries (95 - 105%); the linearity range of standard solution was 0 - 500 μg/L (0, 0.25, 0.5, 1, 5, 10, 25, 50, 100, 250, 500 μg/L, R^2 of standard curve was more than 0.9999); the limit of detection was 0.001 μg/kg; and the limit of quantification was 0.003 μg/kg. The limit of quantification was determined as 10 × standard deviation of the intercept / the average of the slope obtained from seven measurements of the standard solutions. For the analysis of lead concentration, Thallium (^{205}TI) was used as an internal standard for the lead concentration analysis.

Histopathological analysis

For histopathological analysis, the collected organs (liver, spleen, kidney, heart, lung, cerebrum, midbrain, cerebellum, and bone marrow) were fixed in 10% buffered formalin for 48 hours at room temperature and embedded in paraffin. The embedded tissues were sectioned at a thickness of 4 μm and were stained with hematoxylin and eosin (H&E).

Lead staining

Lead staining was performed as previously reported (Turillazzi *et al*., 2013; Neri *et al*., 2007). Deparaffinized and rehydrated tissue sections were incubated with a staining solution containing 2.5 mg/ml sodium rhodizonate (FUJIFILM Wako Chemicals) and 1.67 mg/ml tartaric acid (Sigma-Aldrich) for 1 minute. The sections were counterstained with hematoxylin for 30 seconds, washed with distilled water, dehydrated and mounted. Kidney sections were also stained with acid-fast stain to detect intranuclear lead inclusion body.

Imaging analysis of lead by LA-ICP-MS

For LA-ICP-MS, the collected organs (liver, spleen, kidney, heart, cerebrum, midbrain, and cerebellum) were washed with sterilized phosphate-buffered saline (PBS) to remove blood and then embedded in Tissue-Tek O.C.T. Compound (Sakura Finetek). The embedded tissues were frozen in isopentane, which had been cold with dry ice, allowed to dry and then stored at -80℃. The frozen tissues were sectioned at a thickness of 15 μm using a cryostat Leica CM 3500. Some neighboring sections were cut to a thickness of 8 μm for H&E staining. The sections were analyzed using an LA system (NWR213; esi Japan, Tokyo, Japan, working at a wavelength of 213 nm, pulse duration of 4 ns, and fluence of 0.5-0.6 J cm^{-2}) associated with an ICP-MS 8800 series (Agilent Technology) and scanned by a focused laser beam. Laser spot size, scan speed line and offset

between line were set at 100 μm, 100 μm s^{-1} and 100 μm, respectively. ICP-MS conditions were the following: RF plasma source, 1600 W; He carrier gas, 0.8 L min^{-1}. Measured isotope (dwell time, second) were as follows: ^{13}C (0.005), ^{25}Mg (0.005), ^{31}P (0.005), ^{43}Ca (0.005), ^{55}Mn (0.005), ^{57}Fe (0.005), ^{65}Cu (0.005), ^{66}Zn (0.005), ^{206}Pb (0.01), ^{207}Pb (0.01), ^{208}Pb (0.01). In this analysis, no quantification of Pb was conducted due to lack of suitable reference materials for calibration, however intensity of Pb (and other elements) was normalized to ^{13}C (carbon) intensity as Wu *et al*. (2009), Johnston *et al*. (2019) and others have utilized to normalize the ablation efficiency. From the continuous list of raw pixel values data, elemental images were reconstructed using LA-ICP-MS Image generator house-made software iQquant2 (Kawakami *et al*., 2016).

RESULTS

Clinical signs

Clinical signs of the ducks are summarized in Table 1. Duck-Lead-3 showed mild anorexia and lethargy at 21 days after the lead treatment. The other ducks appeared healthy. The control group did not show any clinical signs.

Clinical signs of the kites are summarized in Table 2. Kite-Lead-2 showed moderate anorexia, lethargy and exercise intolerance at 7 days after the lead administration, and Kite-Lead 1 showed mild anorexia and lethargy at one day after the lead treatment. The other kites appeared healthy. The control group did not show any clinical signs.

Necropsy findings

Necropsy findings of the ducks are summarized in Table 1. An eroded lead pellets remained in the stomach of all the lead-treated ducks except for Duck-Lead-3. Duck-Lead-1, Duck-Lead-2 and

Duck-Control-2 showed focal discolored foci on the surface of the liver. In the Duck-Lead-4, mild hepatomegaly and multifocal yellowish foci on the surface of the liver were observed. In addition, the spleen was mildly swollen, and the right metanephros was defective. Duck-Lead-3, Duck-Control-1 and Duck-Control-3 did not show any gross pathological changes.

Necropsy findings of the kites are summarized in Table 2. No lead pellet was found in the gastrointestinal tract of all the lead-treated kites. Kite-Lead-1 and Kite-Lead-3 showed focal yellowish-white foci on the surface of the liver. The heart of Kite-Lead-2 was mildly fragile. No gross pathological change was noted in the other organs of the lead-treated kites and the control kites.

Histopathological findings

Histopathologic findings of the ducks are summarized in Table 1. Duck-Lead-1, Duck-Lead-2 and Dcuk-Control-3 showed hydropic degeneration of hepatocytes, while Duck-Lead-3, Duck-Lead-4 and Dcuk-Control-1 showed vacuolar degeneration of hepatocytes. All ducks except Duck-Control-2 showed vacuolar degeneration of the renal tubular epithelia. Deposition of amyloid in the hepatic portal area, sinusoid of the liver, and white pulp of the spleen was noted in Duck-Lead-4.

Histopathological findings of the kites are summarized in Table 2. In Kite-Lead-1, an enlargement of the collecting ducts of the kidney and mild hypoplasia of the bone marrow were observed. Mild myocarditis and mild pulmonary congestion were noted in Kite-Lead-2. All kites showed the deposition of lipofuscin in the renal tubular epithelia. Deposition of amyloid in sinusoid of the liver was noted in Kite-Control-2.

Intranuclear lead inclusion body was not found in the acid-fast stained kidney sections of the ducks and kites (data not shown). Lead staining using the sodium rhodizonate reaction was negative in all the ducks and kites (data not shown).

ICP-MS analysis

In the quantitative analysis of lead by ICP-MS, Duck-Lead-3 and Kite-Lead-1 showed the highest lead concentrations in each group. The liver and kidneys showed higher lead concentrations compared with the other organs examined (Table 3). The lead concentrations in untreated control groups were less than 0.01 mg/L or mg/kg (data not shown).

LA-ICP-MS analysis

Tissue distributions of lead were examined in Duck-Lead-3 and Kite-Lead-1 by LA-ICP-MS, as these birds showed the highest lead concentrations. In addition, the cerebrum, midbrain, and cerebellum of Duck-Lead-1, or the cerebrum, midbrain, cerebellum, and heart of Kite-Lead-3 were also examined to confirm the characteristic patterns of lead distribution.

In the lead-exposed duck, diffuse lead accumulation except for veins was noted in the liver (Figure 1A). Connective tissues surrounding veins showed slightly higher intensities. The lumen of the gallbladder also showed lead accumulation. In the spleen, lead accumulation was restricted to the red pulp (Figure 1B). In the kidney, diffuse lead accumulation was observed in the cortex (Figure 1C). The cortical areas surrounding the interlobular veins showed higher intensities compared with the areas around the central veins. Notably, the medullary cones did not show lead accumulation. In the brain, lead accumulated diffusely in the cerebrum (Figure 1D). In the cerebellar cortex, the gray matter showed diffuse lead accumulation, with higher intensities in the

Purkinje cell layer (Figure 1E). In the midbrain, the optic tectum (stratum griseum et fibrosum superficiale, stratum griseum centrale, stratum griseum periventriculare), central gray substance, and oculomotor nerves showed intensive lead accumulation (Figure 1F). Lead accumulation was not observed in the untreated control duck (Figures 1G and 1H).

In the lead-exposed kite, intensive lead accumulation in the hepatic arterial walls was observed in addition to diffuse accumulation in hepatic parenchyma (Figure 2A). In the spleen, the wall of splenic artery showed much higher amount of lead accumulation than those of the red pulp (Figure 2B). In the kidney, the patterns of lead distribution were the same as those of the duck kidney (Figure 2C). Diffuse lead accumulation was observed in the renal cortex, with higher intensities around the interlobular veins. Materials contained in dilated collecting ducts also showed lead signals. In the cerebrum, intensive lead accumulation was noted in the peripheral area of the hyperpallium, hippocampus, and hypothalamus, in addition to diffuse accumulation in parenchyma (Figure 2D). In the cerebellum, lead accumulated diffusely in the gray matter, with higher intensities in the Purkinje cell layer (Figure 2E). In the midbrain, the optic tectum (stratum griseum et fibrosum superficiale, stratum griseum centrale, stratum griseum periventriculare), central gray substance, nucleus mesencephalicus lateralis pars dorsalis, brachium cunjuctivum, and oculomotor nerves showed intensive lead accumulation (Figure 2E). Lead accumulation was not observed in the untreated control kite (Figures 2F and 2G). Thus, the pattens of lead accumulation in the lead-exposed kites were basically similar to those of the lead-exposed ducks, with more prominent lead accumulation in some brain regions, *e.g.*, hyperpallium, hippocampus, hypothalamus, and optic tectum. Meanwhile, the intensive lead accumulation in the arterial wall was characteristic to the lead-exposed kite. The intensive lead accumulation in the arterial wall

was also confirmed in the heart of the lead-exposed kite (Figure 2H). The walls of coronary artery and aorta showed high amount of lead accumulation in addition to those of the cardiac cartilage.

Taking advantage of LA-ICP-MS that enables to visualize the distribution of essential elements in tissue sections, we also examined localization of magnesium, phosphorus, calcium, manganese, iron, copper, zinc at the suborgan level in the lead-exposed ducks and kites. Notably, the distribution of copper was altered in the cerebrum of the lead-exposed ducks (Figure 3). Copper accumulated in the entopallium only in the lead-exposed ducks and not in the control duck or the lead-exposed kites. Localization of the other elements in each organ was not altered by the lead administration (data not shown).

DISCUSSION

In the present study, lead distribution in organs of experimentally lead-exposed ducks and kites were investigated at the suborgan level by LA-ICP-MS. Although almost all of the ducks and kites lacked lead-associated pathological changes due to the low-dosage of lead administration, tissue distribution of lead could be clearly identified. In addition, species differences in lead distribution patterns were also revealed.

In the liver, lead accumulated diffusely in parenchyma in both the duck and kite. This distribution pattern is the same as those in lead-exposed mice (Togao *et al*., 2020). Lead-intoxicated animals show degeneration of hepatocytes and hemosiderosis (Ochiai *et al*., 1993; Jarrar and Taib, 2012; Hegazy and Fouad, 2014). Thus, the diffuse distribution of lead in hepatocytes is compatible with the histopathological changes in lead-intoxicated animals.

In the spleen, lead accumulated only in the red pulp in both the duck and kite. This finding is in line with the report that 95% of lead in blood accumulates in erythrocytes (Hernández-Avila *et al*.,

1998). In addition, hemosiderin-laden (erythrophagocytic) macrophages increase in the red pulp in lead-intoxicated waterfowls (Ochiai *et al*., 1993). It has been reported that lead specifically affects macrophages in the red pulp in lead-exposed mice (Corsetti *et al*., 2017). Therefore, the lead accumulation in the red pulp may reflect the lead accumulation in erythrocytes and erythrophagocytic macrophages.

In the kidneys of the duck and kite, lead accumulated diffusely in the cortical area, particularly around the interlobular veins, without accumulation in the medullary cones. These distribution patterns are different from those observed in lead-exposed mice, in which corticomedullary boundaries show higher amount of lead accumulation than the cortex (Togao *et al*., 2020). Birds and mammals have different kidney structures in terms of nephron, portal system, and stratified cortex and medulla (Morild *et al*., 1985; Harr, 2002). Thus, these structural differences may account for the different lead distribution. Meanwhile, the lack of lead accumulation in the renal medulla is common in both birds and mammals. The appearance of inclusion bodies composed of lead, α-synuclein and metallothionein in the proximal tubules is a histological hallmark of lead-intoxicated animals (Moore and Goyer, 1974; Qu *et al*., 2002; Zuo *et al*., 2009). In addition, lead-intoxicated animals show degeneration and necrosis of the proximal tubules. Therefore, the diffuse lead distribution in the cortical area is in line with the histopathological changes of the lead-intoxicated animals.

In the brain, lead accumulated diffusely in the cerebrum, cerebellar cortex, and midbrain in both the ducks and kites, with higher intensities in the Purkinje cell layer, optic tectum, central gray substance, and oculomotor nerves. In the kites, hippocampus, hyperpallium, and hypothalamus also showed higher amount of lead accumulation. These patterns of lead distribution partially overlap with those of rodents, in which lead preferentially accumulates in hippocampus and the

cerebral cortex (Lefauconnier *et al*., 1983; Al-Shimali *et al*., 2016; Togao *et al*., 2020). In lead-exposed rodents, neuronal damages are mainly observed in hippocampus, the parietal cortex, and Purkinje cells (Sharifi *et al*., 2002; Dribben *et al*., 2011; Gargouri *et al*., 2012; Owoeye and Onwuka, 2016), and lipid peroxidation is noted in thalamus, hippocampus, the parietal cortex and striatum in rats (Villeda-Hernández *et al*., 2001). In birds, lead exposure causes neurological dysfunction like blindness, head tilt, and seizures (Fallon *et al*., 2017). The intensive lead accumulation in the Purkinje cell layer and optic tectum may account for these clinical signs in birds. In addition, the lead accumulation in hippocampus of the kites may associate with the finding that lead exposure has a negative impact on learning and behavior in avian species (Burger and Gochfeld, 2005; Ecke *et al*., 2017). Further studies will be needed to investigate the relationship between the lead distribution in the brain and neurological signs in lead-exposed birds. In addition, the identification of brain cell types which have higher amount of lead will aid to unveil the mechanisms of lead-induced neurotoxicity. For example, astrocytes generate and store glutathione sulfhydryl enzymes that can bind lead, and the interaction between astrocytes and neurons is inhibited by lead through the prevention of glutamate and glycogen metabolisms (Strużyńska *et al*., 2005; Liu *et al*., 2015).

Meanwhile, lead exposure caused copper accumulation in the entopallium of the duck brain. It has been reported that lead administration increases copper concentrations in the brain or in cultured astrocytes (Tiffany-Castiglioni *et al*., 1987; Sierra *et al*., 1989). Lead exposure induces copper uptake by up-regulation of the expression of Cu transporter 1 (CTR1) and reduces copper efflux by down-regulation of the expression of ATPase copper transporting alpha (ATP7A) (Zheng *et al*., 2014). The entopallium is one of the visual centers in the bird brain and a target of the tectofugal visual pathway, *i.e.*, a visual route travels from the eyes to optic tectum to thalamus and

317 then to the entopallium (Karten and Hodos, 1970). The clinical relevance and molecular
318 mechanisms of the copper accumulation in the entopallium of the lead-exposed ducks needs to be
319 investigated in the future.

320 The most striking difference in lead distributions between the ducks and kites was the intensive
321 accumulation in the arterial walls of the kites. In lead-intoxicated eagles, hemorrhage and ischemia
322 caused by fibrinoid necrosis of small and medium caliber arteries are frequently found in the heart,
323 brain, and eyes (Manning *et al*., 2019). Thus, arterial walls may be one of the target organs of lead-
324 poisoning in raptors. Lead exposure causes cardiovascular degeneration also in humans and
325 rodents (Navas-Acien *et al*., 2007; Fiorim *et al*., 2011; Ozturk *et al*., 2014; Nascimento *et al*.,
326 2015). In rats, lead exposure increases the activity of plasma matrix metalloproteinase 9 (MMP9)
327 (92-kDa type IV collagenase) (Nascimento *et al*., 2015), which can digest type IV collagen in the
328 basement membrane of blood vessels and elastin of the tunica media of blood vessels (Wilhelm *et*
329 *al*., 1989; Collier *et al*., 1988; Yasmin *et al*., 2005). Further, lead exposure increases the expression
330 of MMP2 (72-kDa type IV collagenase) and MMP9 in hippocampus and the cerebral cortex of
331 mice, resulting in cerebral vascular lesions (Ning *et al*., 2016). In addition, lead-induced expression
332 of MMP2 and MMP9 affects the blood-brain-barrier permeability through degradation of tight
333 junction proteins (Liu *et al*., 2017). Although the distribution of MMPs in avian species has not
334 been investigated, lead may bind and activate MMP2 and MMP9 in the arterial walls in raptors.
335 The molecular mechanisms of the predisposition to the lead accumulation in the arterial walls in
336 raptors should be investigated in the future.

337 Little is known about the toxicity caused by low-level lead exposure in birds. To date, lead
338 toxicity in birds has only been investigated by high-dose lead exposure (Franson *et al*.,1983;
339 Hoffman *et al*., 1985; Mautino and Bell, 1986; Pain, 1990; Redig *et al*., 1991; Rocke and Samuel,

1991; Ochiai *et al*., 1993; Hiraga *et al*., 2008). In mammals, low-dose lead exposure exerts toxic effects (Dribben *et al*., 2011; Flora *et al*., 2012; Lanphear *et al*., 2018; Rahman *et al*., 2018), and Centers for Disease Control and Prevention (CDC) suggested that the safe blood lead level in humans should be reduced from 10 μg/dL to 5 μg/dL (CDC, 2012). Thus, it is currently considered that previous effect-level 'thresholds' should be abandoned in the field of avian lead poisoning (Pain *et al*., 2019). To reproduce the low-dose lead exposure found in the field, we established a model of low-dose lead exposure in waterfowls and raptors in the present study. Although these birds lacked apparent lead-associated pathological changes, the imaging analysis using LA-ICP-MS clearly identified lead distribution in organs. In addition, the alteration of copper distribution in the brain was also detected by LA-ICP-MS. Thus, the present study will provide useful information to understand the mechanisms of lead poisoning in birds caused by low-level exposure in the field.

CONCLUSIONS

Here we demonstrate detailed lead distribution in organs of experimentally lead-exposed birds and its differences between avian species for the first time. The present study will pave the way for better understanding the cellular processes of lead poisoning and the mechanisms of species differences in susceptibility to lead exposure.

ACKNOWLEDGEMENT

We would like to express our appreciation to all the members of Laboratory of Comparative Pathology and Laboratory of Toxicology, Faculty of Veterinary Medicine, Hokkaido University and the Institute for Raptor Biomedicine Japan for helpful discussions, encouragement and support.

FUNDING

This work was supported by the Grants-in-Aid for Scientific Research from the Ministry of Education, Culture, Sports, Science and Technology of Japan awarded to T. Matsukawa (No. 19H01081), M. Ishizuka (No. 16H0177906, 18K1984708, 18KK028708 and JPMXS0420100620), Y. Ikenaka (No. 18H0413208), and S.M.M. Nakayama (No. 17KK0009, 20K20633). This work was also supported by the foundation of JSPS Bilateral Open Partnership Joint Research Projects (JPJSBP120209902) and the Environment Research and Technology Development Fund (SII-1/3-2, 4RF-1802/18949907) of the Environmental Restoration and Conservation Agency of Japan. We also acknowledge financial support from the Soroptimist Japan Foundation, the Nakajima Foundation, the Sumitomo Foundation, the Nihon Seimei Foundation, act beyond trust, the Japan Prize Foundation, and Triodos Foundation. This research was also supported by JST/JICA, SATREPS (Science and Technology Research Partnership for Sustainable Development; No. JPMJSA1501). The funders had no role in study design, data collection and analysis, decision to publish, or preparation of the manuscript.

REFERENCES

1. Al-Shimali, H., Al-Musaileem, A. F., Rao, M. S. Khan, K. M., 2016. Low-dose exposure to lead during pregnancy affects spatial learning, memory and neurogenesis in hippocampus of young rats. J. Neurol. Neurosci. 7, 1-12.
2. Berny, P., Vilagines, L., Cugnasse, J. M., Mastain, O., Chollet, J. Y., Joncour, G. Razin, M., 2015. VIGILANCE POISON: Illegal poisoning and lead intoxication are the main factors

affecting avian scavenger survival in the Pyrenees (France). Ecotoxicol. Environ. Saf. 118, 71-82.

3. Burger, J. Gochfeld, M., 2005. Effects of lead on learning in herring gulls: an avian wildlife model for neurobehavioral deficits. Neurotoxicology. 26, 615-624.

4. CDC, Advisory Committee on Childhood Lead Poisoning Prevention, 2012. Low level lead exposure harms children: a renewed call for primary prevention. https://www.cdc.gov/nceh/lead/ACCLPP/Final_Document_030712.pdf (accessed 16 March 2021).

5. Collier, I. E., Wilhelm, S. M., Eisen, A. Z., Marmer, B. L., Grant, G. A., Seltzer, J. L., Kronberger, A., He, C. S., Bauer, E. A. Goldberg, G. I., 1988. H-ras oncogene-transformed human bronchial epithelial cells (TBE-1) secrete a single metalloprotease capable of degrading basement membrane collagen. J. Biol. Chem. 263, 6579-6587.

6. Corsetti, G., Romano, C., Stacchiotti, A., Pasini, E. Dioguardi, F. S., 2017. Endoplasmic reticulum stress and apoptosis triggered by sub-chronic lead exposure in mice spleen: a histopathological study. Biol. Trace Elem. Res. 178, 86-97.

7. De Francisco, N., Ruiz Troya, J. D. Agüera, E. I., 2003. Lead and lead toxicity in domestic and free living birds. Avian Pathol. 32, 3-13.

8. Dribben, W. H., Creeley, C. E. Farber, N., 2011. Low-level lead exposure triggers neuronal apoptosis in the developing mouse brain. Neurotoxicology and Teratology, 33, 473-480.

9. Ecke, F., Singh, N. J., Arnemo, J. M., Bignert, A., Helander, B., Berglund, Å. M. M., Borg, H., Bröjer, C., Holm, K., Lanzone, M., Miller, T., Nordström, Å., Räikkönen, J., Rodushkin, I., Ågren, E. Hörnfeldt, B., 2017. Sublethal lead exposure alters movement behavior in free-ranging golden eagles. Environ. Sci. Technol. 51, 5729-5736.

10. Ek, K. H., Morrison, G. M., Lindberg, P. Rauch S., 2004. Comparative tissue distribution of metals in birds in Sweden using ICP-MS and laser ablation ICP-MS. Arch. Environ. Contam. Toxicol. 47, 259-269.
11. Fallon, J. A., Redig P., Miller, T., Lanzone, M. Katzner, T., 2017. Guidelines for evaluation and treatment of lead poisoning of wild raptors. Wildl. Soc. Bull. 41, 205-211.
12. Fiorim, J., Ribeiro, R. F., Silveira, E. A., Padilha, A. S., Vescovi, M., Vinícius A., de Jesus, H. C., Stefanon, I., Salaices, M. Vassallo, D. V., 2011. Low-level lead exposure increases systolic arterial pressure and endothelium-derived vasodilator factors in rat aortas. PLoS One. 6, e17117.
13. Fisher, I. J., Pain, D. J. Thomas, V. G., 2006. A review of lead poisoning from ammunition sources in terrestrial birds. Biol. Conserv. 131, 421-432.
14. Flora, G., Gupta, D. Tiwari, A., 2012. Toxicity of lead: a review with recent updates. Interdiscip. Toxicol. 5, 47-58.
15. Franson, J. C., Sileo, L., Pattee, O. H. Moore, J. F., 1983. Effects of chronic dietary lead in American kestrels (*Falco sparverius*). J. Wildl. Dis. 19, 110-113.
16. Gargouri, M., Ghorbel-Koubaa, F., Bonenfant-Magné, M., Magné, C., Dauvergne, X., Ksouri, R., Krichen, Y., Abdelly, C. El Feki, A., 2012. Spirulina or dandelion-enriched diet of mothers alleviates lead-induced damages in brain and cerebellum of newborn rats. Food Chem. Toxicol. 50, 2303-2310.
17. Harr, K. E., 2002. Clinical chemistry of companion avian species: a review. Vet. Clin. Pathol. 31, 140-151.
18. Hegazy, A. M. S. Fouad, U. A., 2014. Evaluation of lead hepatotoxicity, histological, histochemical and ultrastructural study. Forensic Medicine and Anatomy Research, 2, 70-79.

19. Hernández-Avila, M., Smith, D., Meneses, F., Sanin, L. H. Hu, H., 1998. The influence of bone and blood lead on plasma lead levels in environmentally exposed adults. Environ. Health Perspect. 106, 473-477.
20. Hiraga, T., Ohyama, K., Hashigaya, A., Ishikawa, T., Muramoto, W., Kitagawa, H., Mizuno, N. Teraoka, H., 2008. Lead exposure induces pycnosis and enucleation of peripheral erythrocytes in the domestic fowl. Vet. J. 178, 109-114.
21. Hoffman, D. J., Christian F. J., Pattee, O. H., Bunck, C. M. Murray, H. C., 1985. Biochemical and hematological effects of lead ingestion in nestling American kestrels (*Falco sparverius*). Comp. Biochem. Physiol. C Comp. Pharmacol. Toxicol. 80, 431-439.
22. Honda, K., Lee, D. P. Tatsukawa, R., 1990. Lead poisoning in swans in Japan. Environ. Pollut. 65, 209-218.
23. Ishii, C., Nakayama, S. M. M., Ikenaka, Y., Nakata, H., Saito, K., Watanabe, Y., Mizukawa H., Tanabe S., Nomiyama K., Hayashi T. Ishizuka, M., 2017. Lead exposure in raptors from Japan and source identification using Pb stable isotope ratios. Chemosphere. 186, 367-373.
24. Ishii, C., Nakayama, S. M. M., Kataba, A., Ikenaka, Y., Saito, K., Watanabe, Y., Makino, Y., Matsukawa, T., Kubota, A., Yokoyama, K., Mizukawa, H., Hirata, T. Ishizuka, M., 2018. Characterization and imaging of lead distribution in bones of lead-exposed birds by ICP-MS and LA-ICP-MS. Chemosphere. 212, 994-1001.
25. Jarrar, B. M. Taib, N. T., 2010. Histological and histochemical alterations in the liver induced by lead chronic toxicity. Saudi J. Biol. Sci. 19, 203-210.
26. Johnston, J.E., Franklin, M., Roh, H., Austin, C. Arora, M., 2019. Lead and arsenic in shed deciduous teeth of children living near a lead-acid battery smelter. Environ. Sci. Technol. 53, 6000-6006.

27. Karten, H. J. Hodos, W., 1970. Telencephalic projections of the nucleus rotundus in the pigeon (*Columba livia*). J. Comp. Neurol. 140, 35-51.

28. Kawakami, T., Hokada, T., Sakata, S. Hirata, T., 2016. Possible polymetamorphism and brine infiltration recorded in the garnet-sillimanite gneiss, Skallevikshalsen, Lutzow-Holm Complex, East Antarctica. J. Mineral. Petrol. Sci. 111, 129-143.

29. Lanphear, B. P., Rauch, S., Auinger, P., Allen, R. W. Hornung, R. W., 2018. Low-level lead exposure and mortality in US adults: a population-based cohort study. Lancet Public Health. 3, e177-e184.

30. Lefauconnier, J. M., Bernard, G., Mellerio, F., Sebille, A. Cesarini, E., 1983. Lead distribution in the nervous system of 8-month-old rats intoxicated since birth by lead. Experientia. 39, 1030-1031.

31. Liao, Y., Yu, F., Jin, Y., Lu, C., Li, G., Zhi, X., An, L. Yang, J., 2008. Selection of micronutrients used along with DMSA in the treatment of moderately lead intoxicated mice. Arch. Toxicol. 82, 37-43.

32. Liu, J. T., Dong, M. H., Zhang, J. Q., Bai, Y., Kuang, F. Chen, L. W., 2015. Microglia and astroglia: the role of neuroinflammation in lead toxicity and neuronal injury in the brain. Neuroimmunol. Neuroinflamm. 2, 131-137.

33. Liu, X., Su, P., Meng, S., Aschner, M., Cao, Y., Luo, W., Zheng, G. Liu, M., 2017. Role of matrix metalloproteinase-2/9 (MMP2/9) in lead-induced changes in an in vitro blood-brain barrier model. Int. J. Biol. Sci. 13, 1351-1360.

34. Manning, L. K., Wünschmann, A., Armién, A. G., Willette, M., MacAulay, K., Bender, J. B., Buchweitz, J. P. Redig, P., 2019. Lead intoxication in free-ranging bald eagles (*Haliaeetus leucocephalus*). Vet. Pathol. 56, 289-299.

35. Mautino, M. Bell, J. U., 1986. Experimental lead toxicity in the ring-necked duck. Environ. Res. 41, 538-545.
36. Moore, J. F. Goyer, R. A., 1974. Lead induced inclusion bodies: composition and probable role in lead metabolism. Environ. Health Perspect. 7, 121-127.
37. Morild, I., Bohle, A. Christensen, J. A., 1985. Structure of the avian kidney. Anat. Rec. 212, 33-40.
38. Nascimento, R. A., Mendes, G., Possomato-Vieira, J. S., Gonçalves-Rizzi, V. H., Kushima, H., Delella, F. K. Dias-Junior, C. A., 2015. Metalloproteinase inhibition protects against reductions in circulating adrenomedullin during lead-induced acute hypertension. Basic Clin. Pharmacol. Toxicol. 116, 508-515.
39. Navas-Acien, A., Guallar, E., Silbergeld, E. K. Rothenberg, S. J., 2007. Lead exposure and cardiovascular disease - a systematic review. Environ. Health Perspect. 115, 472-482.
40. Neri, M., Turillazzi, E., Riezzo, I. Fineschi, V., 2007. The determination of firing distance applying a microscopic quantitative method and confocal laser scanning microscopy for detection of gunshot residue particles. Int. J. Legal Med. 121, 287-292.
41. Ning, L., Xing, L., Li, L., Pingan, Z., Mingwu, Q., Qiuyan, Z., Lianjun, S. Y. Zengli, Y., 2016. The expression of MMP2 and MMP9 in the hippocampus and cerebral cortex of newborn under maternal lead exposure. Exp. Biol. Med. 241, 1811-1818.
42. Ochiai, K., Jin, K., Goryo, M., Tsuzuki, T. Itakura, C., 1993. Pathomorphologic findings of lead poisoning in white-fronted geese (*Anser alhifrons*). Vet. Pathol. 30, 522-528.
43. Owoeye, O. Onwuka, S. K., 2016. Lead toxicity: effect of *Launaea taraxacifolia* on the histological and oxidative alterations in rat regio III cornu ammonis and cerebellum. Anat. J. Africa, 5, 783-794.

44. Ozturk, M. T., Yavuz, B., Ozkan, S., Ayturk, M., Akkan, T., Ozkan, E., Tutkun, E. Yilmaz, Ö. H., 2014. Lead exposure is related to impairment of aortic elasticity parameters. J. Clin. Hypertens. 16 (11), 790-793.
45. Pain, D. J., 1990. Lead shot ingestion by waterbirds in the Camargue, France: an investigation of levels and interspecific differences. Environ. Pollut. 66, 273-285.
46. Pain, D. J., Mateo, R. Green, R. E., 2019. Effects of lead from ammunition on birds and other wildlife: a review and update. Ambio. 48, 935-953.
47. Qu, W., Diwan, B. A., Liu, J., Goyer, R. A., Dawson, T., Horton, J. L., Cherian, M. G. Waalkes, M. P., 2002 The metallothionein-null phenotype is associated with heightened sensitivity to lead toxicity and an inability to form inclusion bodies. Ame. J. Pathol. 160, 1047-1056.
48. Rahman, A., Khan, K. M. Rao, M. S., 2018. Exposure to low level of lead during preweaning period increases metallothionein-3 expression and dysregulates divalent cation levels in the brain of young rats. Neurotoxicology. 65, 135-143.
49. Redig, P. T., Lawler, E. M., Schwartz, S., Dunnette, J. L., Stephenson, B. Duke, G. E., 1991. Effects of chronic exposure to sublethal concentrations of lead acetate on heme synthesis and immune function in red-tailed hawks. Arch. Environ. Contam. Toxicol. 21, 72-77.
50. Rocke, T. E. Samuel, M. D., 1991. Effects of lead shot ingestion on selected cells of the mallard immune system. J. Wildl. Dis. 27, 1-9.
51. Rogan, W. J., Reigart, J. R. Gladen, B. C., 1986. Association of amino levulinate dehydratase levels and ferrochelatase inhibition in childhood lead exposure. J. Pediatr. 109, 60-64.
52. Saito, K., 2009. Lead poisoning of Steller's sea eagle (*Haliaeetus pelagicus*) and White-tailed eagle (*Haliaeetus albicilla*) caused by the ingestion of lead bullets and slugs, in Hokkaido, Japan. In R.T. Watson, M. Fuller, M. Pokras and W.G. Hunt (Eds.). Ingestion Lead from

Spent Ammunition: Implications for Wildlife and Humans pp. 302-309. Idaho: Peregrine Fund.

53. Scheuhammer, A. M. Norris, S. L., 1996. The ecotoxicology of lead shot and lead fishing weights. Ecotoxicology. 5, 279-295.

54. Sharifi, A. M., Baniasadi, S., Jorjani, M., Rahimi, F. Bakhshayesh, M., 2002. Investigation of acute lead poisoning on apoptosis in rat hippocampus in vivo. Neurosci. Lett. 329, 45-48.

55. Sierra, E. M., Rowles, T. K., Martin, J., Bratton, G. R., Womac, C. and Tiffany-Castiglioni, E., 1989. Low level lead neurotoxicity in a pregnant guinea pigs model: neuroglial enzyme activities and brain trace metal concentrations. Toxicology. 59, 81-96.

56. Strużyńska, L., Chalimoniuk, M. Sulkowski, G., 2005. The role of astroglia in Pb-exposed adult rat brain with respect to glutamate toxicity. Toxicology. 212, 185-194.

57. Tiffany-Castiglioni, E., Zmudzki, J., Wu, J. N. Bratton, G. R., 1987. Effects of lead treatment on intracellular iron and copper concentrations in cultured astroglia. Metab. Brain Dis. 2, 61-79.

58. Togao, M., Nakayama, S. M. M., Ikenaka, Y., Mizukawa, H., Makino, Y., Kubota, A., Matsukawa, T., Yokoyama, K., Hirata, T. Ishizuka, M., 2020. Bioimaging of Pb and STIM1 in mice liver, kidney and brain using laser ablation inductively coupled plasma mass spectrometry (LA-ICP-MS) and immunohistochemistry. Chemosphere. 238, 124581.

59. Turillazzi, E., Di Peri, G. P., Nieddu, A., Bello, S., Monaci, F., Neri, M., Pomara, C., Rabozzi, R., Riezzo, I. Fineschi, V., 2013. Analytical and quantitative concentration of gunshot residues (Pb, Sb, Ba) to estimate entrance hole and shooting-distance using confocal laser microscopy and inductively coupled plasma atomic emission spectrometer analysis: an experimental study. Forensic Sci. Int. 231, 142-149.

60. Villeda-Hernández, J., Barroso-Moguel, R., Méndez-Armenta, M., Nava-Ruíz, C., Huerta-Romero, R. Ríos, C., 2001. Enhanced brain regional lipid peroxidation in developing rats exposed to low level lead acetate. Brain Res. Bull. 55, 247-251.

61. Wilhelm, S. M., Collier, I. E., Marmer, B. L., Eisen, A. Z., Grant, G. A. Goldberg, G. I., 1989. SV40-transformed human lung fibroblasts secrete a 92-kDa type IV collagenase which is identical to that secreted by normal human macrophages. J. Biol. Chem. 264, 17213-17221.

62. Wu, B., Zoriy, M., Chen, Y. Becker, J. S., 2009. Imaging of nutrient elements in the leaves of *Elsholtzia splendens* by laser ablation inductively coupled plasma mass spectrometry (LA-ICP-MS). Talanta. 78, 132-137.

63. Yabe, J., Nakayama, S. M. M., Ikenaka, Y., Yohannes, Y. B., Bortey-Sam, N., Oroszlany, B., Muzandu, K., Choongo, K., Kabalo, A. N., Ntapisha, J., Mweene, A., Umemura, T. Ishizuka, M., 2015. Lead poisoning in children from townships in the vicinity of a lead-zinc mine in Kabwe, Zambia. Chemosphere. 119, 941-947.

64. Yasmin, S. W., McEniery, C. M., Dakham, Z., Pusalkar, P., Maki-Petaja, K. Ashby, M. J., Cockcroft, J. R. Wilkinson, I. B., 2005. Matrix metalloproteinase-9 (MMP-9), MMP-2, and serum elastase activity are associated with systolic hypertension and arterial stiffness. Arterioscler. Thromb. Vasc. Biol. 25, 372-378.

65. Zheng, G., Zhang, J., Xu, Y., Shen, X., Song, H., Jing, J., Luo, W., Zheng, W. Chen, J., 2014. Involvement of CTR1 and ATP7A in lead (Pb)-induced copper (Cu) accumulation in choroidal epithelial cells. Toxicol. Lett. 225, 110-118.

66. Zuo, P., Qu, W., Cooper, R. N., Goyer, R. A., Diwan, B. A. Waalkes, M. P., 2009. Potential role of α-synuclein and metallothionein in lead-induced inclusion body formation. Toxicol. Sci. 111, 100-108.

569 **Table 1.** Summary of clinical signs, necropsy findings and histopathological findings of the ducks

Duck	Clinical signs	Necropsy findings	Histopathological findings
Lead-1	None	Liver: focal dark red foci	Liver: hydropic degeneration of hepatocytes, diffuse, moderate; subcapsular hemorrhage and edema, focal, mild Kidney: vacuolar degeneration of the renal tubules, diffuse, mild
Lead-2	None	Liver: focal yellowish-white foci	Liver: hydropic degeneration of hepatocytes, diffuse, moderate Kidney: vacuolar degeneration of the renal tubules, diffuse, mild
Lead-3	Mild anorexia and lethargy	None	Liver: vacuolar degeneration of hepatocytes, diffuse, moderate Kidney: vacuolar degeneration of the renal tubules, multifocal, mild
Lead-4	None	Liver: mild hepatomegaly and multifocal yellowish foci Spleen: mild splenomegaly Kidney: defect of the right metanephros	Liver: deposition of amyloid within the hepatic portal area, sinusoid and white pulp, diffuse, moderate; vacuolar degeneration of hepatocytes, diffuse, moderate Kidney: vacuolar degeneration of the renal tubules, diffuse, mild
Control-1	None	None	Liver: vacuolar degeneration of hepatocytes, diffuse, moderate Kidney: vacuolar degeneration of the renal tubules, multifocal, mild
Control-2	None	Liver: focal white foci	None
Control-3	None	None	Liver: vacuolar degeneration of hepatocytes, diffuse, moderate Kidney: vacuolar degeneration of the renal tubules, multifocal, mild

570

571 **Table 2.** Summary of clinical signs, necropsy findings and histopathological findings of the kites

Kite	Age and sex	Clinical signs	Necropsy findings	Histopathological findings
Lead-1	6 y, female	Mild anorexia and lethargy	Liver: focal yellowish-white foci	Kidney: deposition of lipofuscin in the renal tubules, diffuse, mild; enlargement of the collecting ducts, moderate Bone marrow: hypoplasia, mild
Lead-2	2 y, female	Moderate anorexia, lethargy and exercise intolerance	Heart: mild fragileness	Kidney: deposition of lipofuscin in the renal tubules, diffuse, mild Heart: myocarditis, lymphocytic, focal, mild Lung: pulmonary congestion, diffuse, mild
Lead-3	2 y, male	None	Liver: focal yellowish-white foci	Kidney: deposition of lipofuscin in the renal tubules, diffuse, mild
Control-1	6 y, female	None	None	Kidney: deposition of lipofuscin in the renal tubules, diffuse, mild
Control-2	3 y, female	None	None	Kidney: deposition of lipofuscin in the renal tubules, diffuse, mild Spleen: deposition of amyloid within the splenic sinusoid, focal

572

573 **Table 3.** Lead concentrations in the duck and kite organs

Organ	Duck-Lead-3 [a]	Duck-Lead-1	Kite-Lead-1	Kite-Lead-3
Blood [b]	2.95	—	0.99	—
Liver	6.18	—	1.70	—
Spleen	2.80	—	0.35	—
Pronephros	4.89	—	4.90	—
Mesonephros	5.41	—	3.04	—
Metanephros	5.80	—	4.15	—
Cerebrum	0.68	0.18	0.53	0.24
Midbrain	0.81	0.32	0.76	1.52
Cerebellum	0.93	0.73	0.63	0.69
Heart	—	—	—	0.03

574 [a] Data are expressed as mg/L in blood or mg/kg in wet weight in the other organs.

575 [b] Lead concentration in blood at 28 d after the lead administration.

576

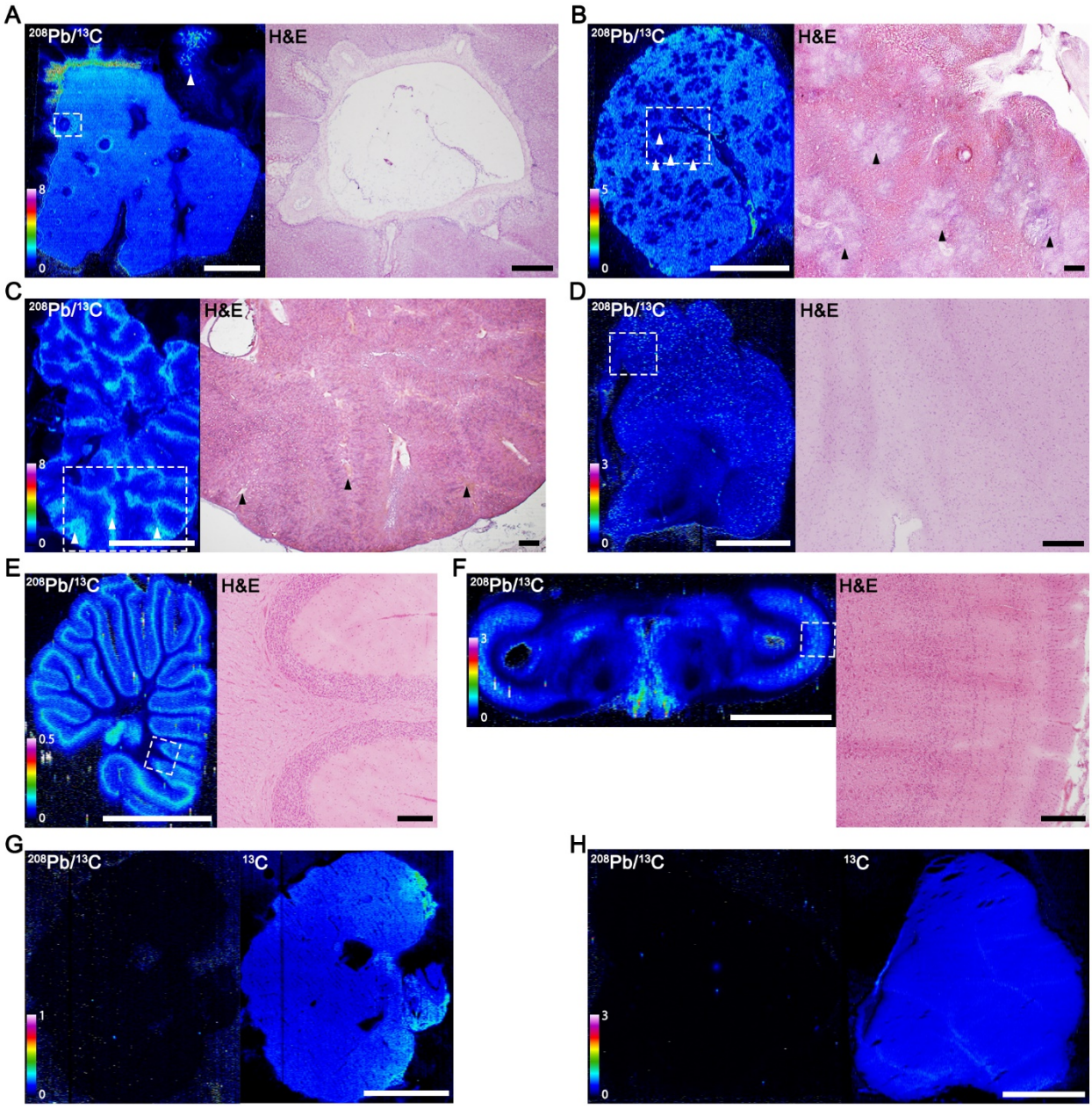

577 **Figure 1.** Lead distribution in the duck organs. (A) Lead accumulated diffusely in the liver. Lead
578 signals were also observed in the gallbladder (arrowhead). Duck-Lead-3. (B) Lead accumulated in
579 the red pulp of the spleen. The white pulp (arrowheads) lacked lead accumulation. Duck-Lead-3.
580 (C) Lead accumulated diffusely in the cortical area of the kidney, with intensive accumulation
581 around the interlobular veins (arrowheads). Duck-Lead-3. (D-F) Lead accumulated diffusely in the

582 cerebrum (D, Duck-Lead-3), cerebellar cortex (E, Duck-Lead-1), and midbrain (F, Duck-Lead-3).
583 The Purkinje cell layer, optic tectum, central gray matter, and oculomotor nerves showed higher
584 amount of lead accumulation. (G, H) Lead accumulation was not observed in the organs of the
585 untreated control duck (G, spleen; H, cerebrum; Duck-Control-3). The areas enclosed by the
586 dashed lines are shown in the H&E images. Scale bars: 5 mm in LA-ICP-MS images and 500 μm
587 in H&E images.

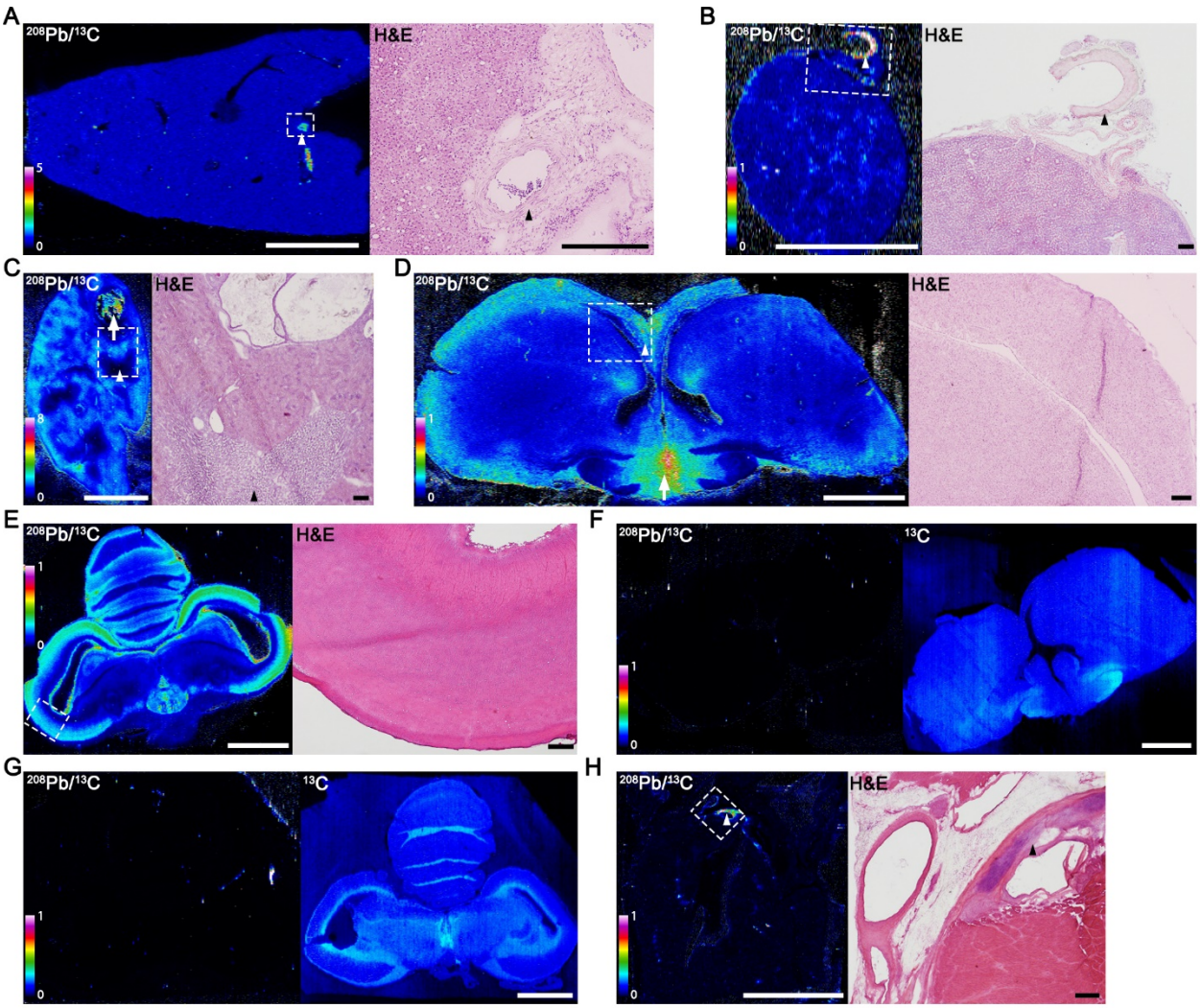

588 **Figure 2.** Lead distribution in the kite organs. (A) Lead accumulated diffusely in the liver, with
589 intensive accumulation in the arterial walls (arrowheads). Kite-Lead-1. (B) Lead accumulated in
590 the red pulp of the spleen, with intensive accumulation in the arterial walls (arrowheads). Kite-
591 Lead-1. (C) Lead accumulated diffusely in the cortical area of the kidney. Lead accumulated also
592 in the dilated collecting ducts (arrow). The medullary cones (arrowheads) lacked lead
593 accumulation. Kite-Lead-1. (D) Lead accumulated diffusely in the cerebrum, with intensive
594 accumulation in the periphery of the hyperpallium, hippocampus (arrowhead), and hypothalamus
595 (arrow). Kite-Lead-1. (E) Lead accumulated diffusely in the cerebellar cortex and midbrain, with

intensive accumulation in the Purkinje cell layer, optic tectum, central gray matter, nucleus mesencephalicus lateralis pars dorsalis, brachium cunjuctivum, and oculomotor nerves. Kite-Lead-3. (F, G) Lead accumulation was not observed in the organs of the untreated control kite (F, cerebrum; G, cerebellum and midbrain; Kite-Control-2). (H) Lead accumulated in the arterial walls of the heart in addition to the cardiac cartilage (arrowheads). Kite-Lead-3. The areas enclosed by the dashed lines are shown in the H&E images. Scale bars: 5 mm in LA-ICP-MS images and 500 μm in H&E images.

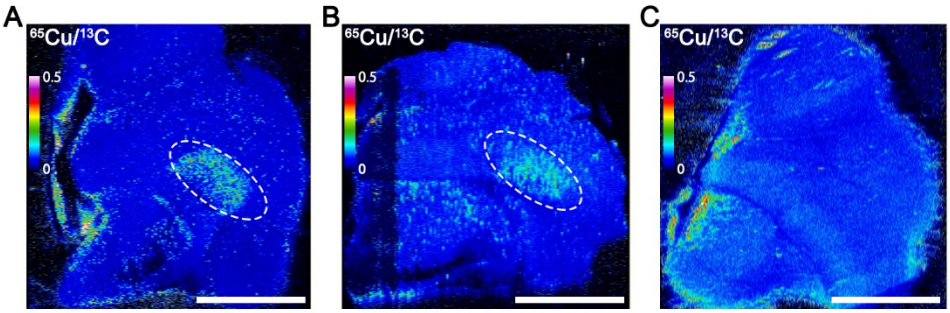

603 **Figure 3.** Copper distribution in the duck brains. (A, B) Copper accumulated in the entopallium
604 (encircled by the dashed lines) of the lead-exposed ducks (A, Duck-Lead-3; B, Duck-Lead1). (C)
605 Copper accumulation in the entopallium was not observed in the untreated control duck (Duck-
606 Control-3). Scale bars: 5 mm.